Chemical Engineering Science 63 (2008) 4035 – 4044

Contents lists available at ScienceDirect

Chemical Engineering Science

journal homepage: www.elsevier.com/locate/ces

Liquid–liquid two-phase flow patterns and mass transfer characteristics in rectangular glass microreactors

Anne-Laure Dessimoz[a], Laurent Cavin[b], Albert Renken[a], Lioubov Kiwi-Minsker[a,*]

[a]Ecole Polytechnique Fédérale de Lausanne, GGRC, ISIC-SB, Station 6, CH-1015 Lausanne, Switzerland
[b]Givaudan Suisse SA, CH-1214 Vernier, Switzerland

ARTICLE INFO

Article history:
Received 4 October 2007
Received in revised form 30 April 2008
Accepted 2 May 2008
Available online 15 May 2008

Keywords:
Microstructure
Multiphase flow
Hydrodynamics
Flow pattern
Mass transfer
Capillary/Reynolds numbers

ABSTRACT

The flow of two immiscible fluids was investigated in rectangular glass microchannels with equivalent diameters of 269 and 400 μm. Deionised water, dyed toluene and hexane were selected as probe fluids. Flow patterns were obtained for Y- and T-junction of two micro-channels and monitored by a photo-camera. Volumetric velocities of water and organic phase varied between 1 and 6 ml/h. The formation mechanism of slug and parallel flow was studied and the mass transfer performances of two flow patterns were compared. The shape of the interface between the immiscible liquids was controlled by a competition between the viscous forces and the local interfacial tension. The flow patterns could be correlated with the mean Capillary and Reynolds numbers. The mass transfer coefficients for parallel and slug flow were determined using instantaneous neutralisation (acid–base) reaction. The two flow patterns showed the same global volumetric mass transfer coefficients in the range of $0.2–0.5\,s^{-1}$, being affected mainly by the base concentration in water for parallel flow and by the linear velocity in the case of the slug flow.

1. Introduction

Intensification of chemical processes aiming at the effective use of raw materials and energy implies miniaturisation of chemical reactors. Microstructured reactors (MSR) are systems with a well-defined structure of channels with an internal diameter in the range of 10–500 μm (Löwe and Ehrfeld, 1999). Due to the small diameters of the channels and the high specific surface area of MSR (in the order of $10,000–50,000\,m^2/m^3$, Jähnisch et al., 2004), high heat transfer performance can be achieved with heat transfer coefficients up to $25,000\,W/(m^2\,K)$ (Ehrfeld et al., 2000). Moreover, the heat exchanger is often integrated within the reactor allowing efficient control of the highly exothermic or endothermic reactions. In the case of multiphase systems, the specific interface is also drastically increased in comparison with traditional reactors. The specific interfacial area of multiphase systems can be obtained in the range of $5000–30,000\,m^2/m^3$ (Ehrfeld et al., 2000). Therefore, microreactors allow an intensification of the fast and strongly exothermic or endothermic reactions as shown recently by Lomel et al. (2006) for the case of organometallic synthesis. Other important characteristics of MSR are the narrow residence time distribution and the easy scale-up with inherent reactor safety (Kiwi-Minsker and Renken, 2005). All these advantages warrant the study of microreactors and their use for production of chemicals. The trend in this direction is accelerating at the present time (Hessel and Löwe, 2005).

In order to define the reaction conditions and to design an MSR for a specific chemical transformation, detailed knowledge of the hydrodynamics in the microchannels is necessary. Controlled hydrodynamics allow to decrease the pressure drop, to improve the mass transfer and to facilitate the product separation from the reaction mixture. The common modes of interface in the case of liquid–liquid two-phase flow are "slug flow" (Fig. 1A) and "parallel flow" (Fig. 1B). In the case of slug flow, two mechanisms are known to be responsible for the mass transfer between two fluids: (a) internal circulation (Burns and Ramshaw, 2001; Dummann et al., 2003; Kashid et al., 2005) takes place within each slug and (b) the concentration gradients between adjacent slugs lead to the diffusion between the phases. In the case of parallel pattern, the flow is laminar and the transfer of molecules between the two phases is supposed to occur only by diffusion.

The main problem in the control of flow pattern is due to the flow dependence on the experimental parameters like: the linear velocity (Burns and Ramshaw, 2001), the ratio of the phases, the fluid properties (Burns et al., 1998; Burns and Ramshaw, 1999), the channel geometries (Kashid and Agar, 2007) and the construction material (Ahmed et al., 2006) of the microreactor. Therefore, all these parameters must be considered simultaneously. In practice, flow pattern maps are used to define the influence of different parameters on the

* Corresponding author.
E-mail address: lioubov.kiwi-minsker@epfl.ch (L. Kiwi-Minsker).

0009-2509/$ - see front matter © 2008 Elsevier Ltd. All rights reserved.
doi:10.1016/j.ces.2008.05.005

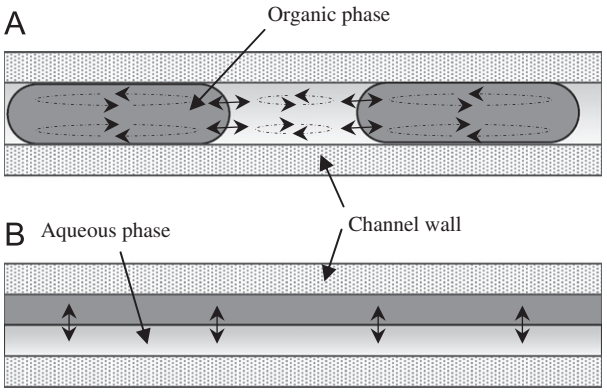

Fig. 1. Types of liquid–liquid two-phase flow patterns in glass microreactors: (A) slug flow; (B) parallel flow.

Table 1
Dimensionless numbers

Reynolds number	$\frac{\text{Inertial forces}}{\text{Viscous forces}}$	$Re = \frac{\rho \cdot u \cdot d_H}{\mu}$
Weber number	$\frac{\text{Inertial forces}}{\text{Liquid–liquid surface tension}}$	$We = \frac{u^2 \cdot d_H \cdot \rho}{\sigma}$
Capillary number	$\frac{\text{Viscous forces}}{\text{Liquid–liquid surface tension}}$	$Ca = \frac{\mu \cdot u}{\sigma}$

hydrodynamics. In so-called flow pattern maps, the axes represent the superficial velocities or the volumetric flow rates of both phases and the flow patterns are plotted with distinct markers. Kashid and Agar (2007) made experiments in Y-shaped PTFE capillary microreactors with a chemical inert system containing water and cyclohexane. The effects of the linear velocity, the channel diameter and the ratio of the volumetric flow rates on the stability of the slug flow regime were represented in a flow pattern map. Zhao et al. (2006) investigated the stability of different flow patterns using a T-junction rectangular microreactor made of PMMA with deionised water and kerosene. In the flow pattern map, the phase Weber numbers (Table 1) were used. The stability domains of the different flow patterns depend on the flow ratio and the volumetric flow rates. However, the model cannot be applied to different geometries of microchannels and to other fluids since it is valid only for the specific fluid system in the specific microreactor. Tice et al. (2004) analysed the conditions required to form slugs of aqueous reagents in flows of immiscible carrier fluid within rectangular microreactor. Flow pattern maps presented the water fraction plotted against the Capillary numbers (Table 1). The influence of the fluid viscosity, linear velocity and the ratio of the phases on the stability of slug flow were studied. However, systematic experimental study of the effect of fluid properties (ρ, σ, μ) on flow patterns stability has not been reported.

In direct link with the hydrodynamics, the mass transfer is of particular importance because microstructured devices are mostly applied for reacting systems. Parallel flow and slug flow form a well-defined environment for mass transfer during multiphase chemical reactions. The internal circulation that arises in slugs when they move through the channel have been described and numerical models of mass transfer between slugs have been developed (Dummann et al., 2003; Harries et al., 2003; Kashid et al., 2005). However, only Burns and Ramshaw (2001) provide data on mass transfer performance during chemical reaction based on experimental results for the slug flow regime without wall film formation. The mass transfer characteristics for the parallel flow have not been reported so far. Moreover, no clear mathematical description of the mass transfer process is available for the two flow patterns.

The objective of the present work is to determine the influence of the fluid properties on liquid–liquid two-phase flow patterns in Y- and T-shaped glass microchannels. Moreover, the mass transfer performance for the parallel and slug flow was studied using an instantaneous neutralisation reaction. A mathematical description based on a film model is suggested to rationalise the observed results.

2. Experimental

2.1. Materials

The experiments were carried out with a Y- or a T-junction glass microreactor (MIKROGLAS, Mainz, D) placed in the same set-up shown in Fig. 2. The glass unit was fixed in an aluminium frame. The frame pressed the connection tubes with fittings (ERCATECK P-200Nx and P-245x) onto the glass surface. All the connection tubes were 1.5 mm outer diameter and 0.6 mm inner diameter PTFE tubes. The two immiscible liquids were introduced inside the glass microreactor by two syringe pumps (ISMATEC kdScientific 100). The behaviour of the fluids in the microchannel was followed under a light source with camera-snapshots (photo camera Panasonic, Lumix DMC-LX1 or Canon, EOS 350D).

2.2. Characterisation of liquid–liquid two-phase flow patterns

The influence of the fluid properties on two-phase flow patterns was investigated in each microreactor using deionised water and toluene. Solutes were added in both phases in order to change the density, the viscosity and the interfacial tension of the fluid system. Three series of experiments were executed with the following fluids: (1) water and toluene, (2) water with NaOH 0.15 M and toluene, (3) water and toluene with CCl_3COOH 0.6 M. For the visualisation of the flow, bromothymol blue was added to the aqueous phase or Sudan III to the organic phase. In each series of experiments, the volumetric flow rate of each phase was varied between 1 and 6 ml/h. All experiments were performed at ambient temperature and pressure. In order to verify the reproducibility of the experiments, two camera-snapshots were taken for each flow and repeated twice.

2.3. Determination of mass transfer coefficients

For the determination of the global mass transfer coefficient ($K_{1,org}$) in slug flow and in parallel flow, the neutralisation (Eq. (1)) was used as a model reaction. The reaction is instantaneous and therefore, is controlled by mass transfer. Burns and Ramshaw (2001) used acetic acid. The trichloroacetic acid applied in this study is a strong acid and gives a colour change at pH 7 due to bromothymol blue used as an indicator.

$$CCl_3COOH_{org} + NaOH_{aqu} \rightarrow CCl_3COO^{-}Na^{+}_{aqu} + H_2O \quad (1)$$

A saturated solution of bromothymol blue in deionised water was used to prepare aqueous solutions containing NaOH from 0.1 to 0.3 M. The trichloroacetic acid was dissolved in toluene or hexane with the concentration of 0.6 M. In some experiments, Sudan III was added to the organic phase for flow visualisation. Experiments were carried out in two microreactors with different concentrations of NaOH in the aqueous phase (see Table 2). For each series of experiments, the total linear velocity was varied between 3 and 46 mm/s (2–12 ml/h) and the ratio of the organic/aqueous phase was kept constant 1:1.

Sodium hydroxide is not soluble in the organic phase whereas trichloroacetic acid is soluble in water. Therefore, the trichloroacetic acid has to diffuse through the interface to react with NaOH. The reaction leads to a colour change (blue → yellow) in the aqueous phase which takes place at pH 7 and indicates the end of the neutralisation reaction.

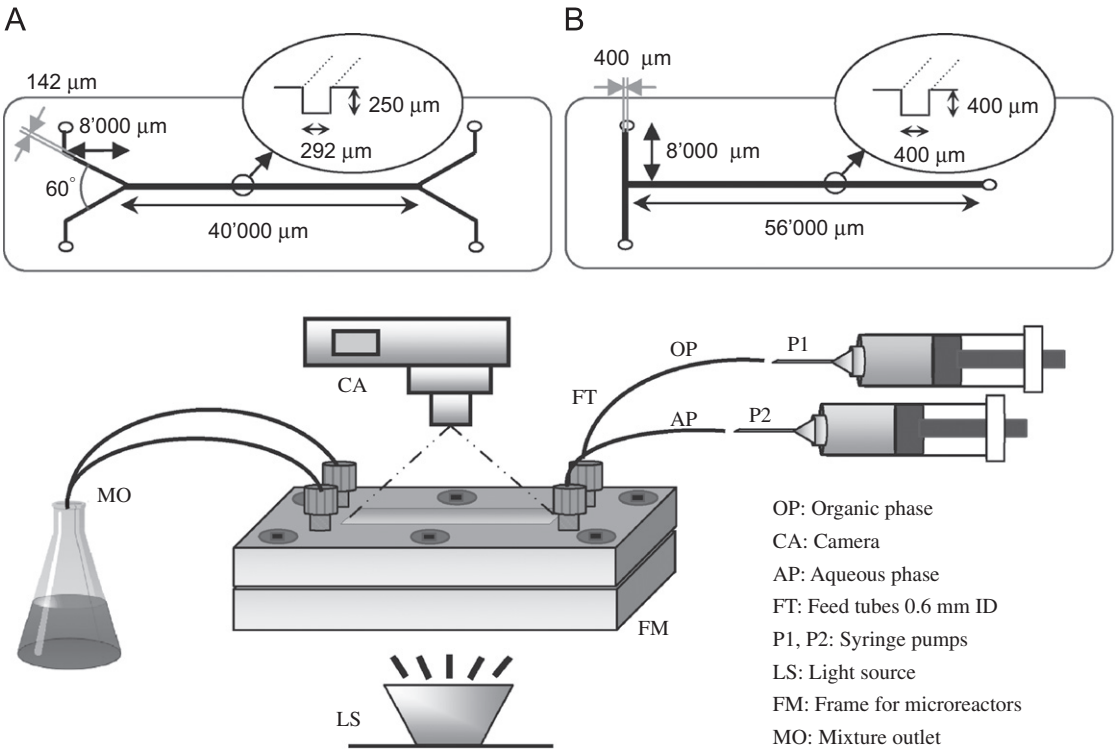

Fig. 2. Scheme of experimental set-up: (A) Y-shaped glass microreactor; (B) T-shaped glass microreactor.

Table 2
Series of experiments performed in the two microreactors with different concentrations of NaOH in the aqueous phase

	C(NaOH) [M]	C(CCl_3COOH) [M]	Organic solvent
Y-microreactor	0.1	0.6	Toluene
	0.15	0.6	Toluene
	0.2	0.6	Toluene
T-microreactor	0.15	0.6	Hexane
	0.2	0.6	Hexane
	0.3	0.6	Hexane

Considering the microreactor as an ideal plug flow reactor, the mass balance under steady state conditions can be expressed as:

$$\frac{dC_i}{d\tau_R} = R_i \tag{2}$$

where τ_R is the time needed to complete the neutralisation reaction. As mentioned above, the reaction is instantaneous and the rate-limiting step is the mass transfer of the trichloroacetic acid. The molar flux of the acid from the organic to the aqueous phase can be expressed by (Trambouze and Euzen, 2002):

$$J_1 = K_{1,org} \cdot (C_{1,org} - C^E_{1,org}) \tag{3}$$

where J_1 is the molar flux of trichloroacetic acid, $K_{1,org}$ is the global mass transfer coefficient from organic to aqueous phase, $C_{1,org}$ is the acid concentration in the organic phase and $C^E_{1,org}$ is the acid concentration at the interface in equilibrium with the aqueous phase.

The rate of disappearance of trichloroacetic acid can be expressed as:

$$-R_1 = J_1 \cdot a = K_{1,org} \cdot (C_{1,org} - C^E_{1,org}) \cdot a \tag{4}$$

Due to the instantaneous reaction taking place in the aqueous phase, the concentration of the acid, $C_{1,aqu}$, becomes zero close to the interface. As a consequence:

$$C^E_{1,org} = m \cdot C_{1,aqu} = 0 \Rightarrow -R_1 = K_{1,org} \cdot C_{1,org} \cdot a \tag{5}$$

Therefore, the mass balance can be rewritten as:

$$\frac{dC_i}{d\tau_R} = -K_{1,org} \cdot a \cdot C_{1,org} \tag{6}$$

The integration gives the global volumetric mass transfer coefficient:

$$K_{1,org} \cdot a = -\frac{1}{\tau_R} \cdot \ln\left(\frac{C_{1,org}}{C_{1,org0}}\right) \tag{7}$$

The distance along the microchannel before the colour change was measured to calculate the time τ_R. Moreover, the colour change appears at pH 7 and corresponds to an amount of acid transferred to the aqueous phase being equivalent to the initial amount of NaOH. So, the acid concentration in the organic phase after the neutralisation reaction is given by:

$$C_{1,org} = C_{1,org0} - C_{2,aqu0} \quad \text{with } Q_{org} = Q_{aqu} \tag{8}$$

3. Results and discussions

3.1. Liquid–liquid two-phase flow patterns in glass microreactors

In the Y-shaped microreactor, the water and toluene system leads to a parallel flow for all volumetric flow rates. The addition of NaOH in the aqueous phase increases the viscosity, the density of water (Vazquez et al., 1996) and the interfacial tension leading to slug flow observed for all flow rates. The effect of acid addition to organic phase was also investigated. However, the CCl_3COOH is soluble in water and diffuses through the interface influencing the properties

of the aqueous phase. The trichloroacetic acid increases the density and the viscosity of water (Lide, 2007), but in contrast to the NaOH, it decreases the interfacial tension between water and toluene resulting in a parallel flow observed for all the flow rates. The values of the interfacial tension corresponding to the addition of acid and base were calculated from the data reported for the water/air surface tension (Lide, 2007; Weast, 1971), via extrapolation. The solvents properties used during the present work are summarised in Table 3.

For the T-shaped microreactor the same experiments were carried out. The water/toluene system forms a slug flow, which is stabilised by the addition of NaOH. The addition of CCl_3COOH gives two types of flow patterns. The parallel flow appears with an increase of the linear velocity. A typical flow pattern map for T-shaped microreactor is shown in Fig. 3.

In summary, the main parameters varied are the linear velocity and the interfacial tension. The results show that an increase of the interfacial tension is favourable for slug flow and that a decrease of the interfacial tension results in parallel flow. The parallel flow is also observed with an increase of the linear velocity. These experiments confirm that the physical properties of fluids influence the observed flow pattern. The theory behind these observations is discussed in the next section and will rationalise the experimental results obtained.

Table 3
Characteristics of the solvents at 20 °C

	ρ [kg/m^3]	μ [Pa s]	$\sigma_{water/liquid}$ [kg/s^2]
Water	998.2	0.001	
Toluene	866.7	0.00059	0.0371
Hexane	659.4	0.0003	0.0511

3.2. Analysis of the flow patterns based on Capillary and Reynolds numbers

Most of the microfluidic devices operate at low Reynolds number. The Navier–Stokes equation is linear and the flow is laminar. In the case of multiphase systems, the Reynolds numbers are low, but the flow can be nonlinear due to interactions at the interface between the immiscible fluids (Thorsen et al., 2001). In the case of two-phase flow in microchannels, the interfacial tension ($\sim \sigma/d$) and the viscous forces ($\sim \mu \cdot u/d$) control the flow patterns because they depend on the channel diameter (Ahmed et al., 2006; Akbar et al., 2003; Kreutzer et al., 2005). The effects of gravity ($\sim \rho \cdot g \cdot H$) and inertia ($\sim \rho \cdot u^2$) become negligible at the micrometer scale (Atencia and Beebe, 2005). The competition between the main forces can be quantified using dimensionless numbers (Akbar et al., 2003; Squires and Quake, 2005).

In order to define quantitatively the influence of the interfacial tension and of the linear velocity on the flow patterns, the Capillary and the Reynolds numbers (Table 1) were calculated for all the experiments with equal volumetric flow rates of the two phases. The Capillary and Reynolds numbers were calculated for each phase and then the mean value between the two phases was considered. Mean dimensionless numbers were used to take in consideration the influence of the properties of both phases on flow patterns. The Capillary number was chosen because the viscous forces and the interfacial tension are the dominating forces in microfluidic devices.

For the Y-shaped microreactor (Fig. 4A), the addition of NaOH decreases slightly the Capillary number in comparison to the water/toluene system due to the effect of the interfacial tension for the identical linear velocity. Therefore, the addition of NaOH in the aqueous phase increases the interfacial tension in comparison to viscous forces. If the flow of two immiscible fluids is dominated by the interfacial tension, slugs are formed because the interfacial tension

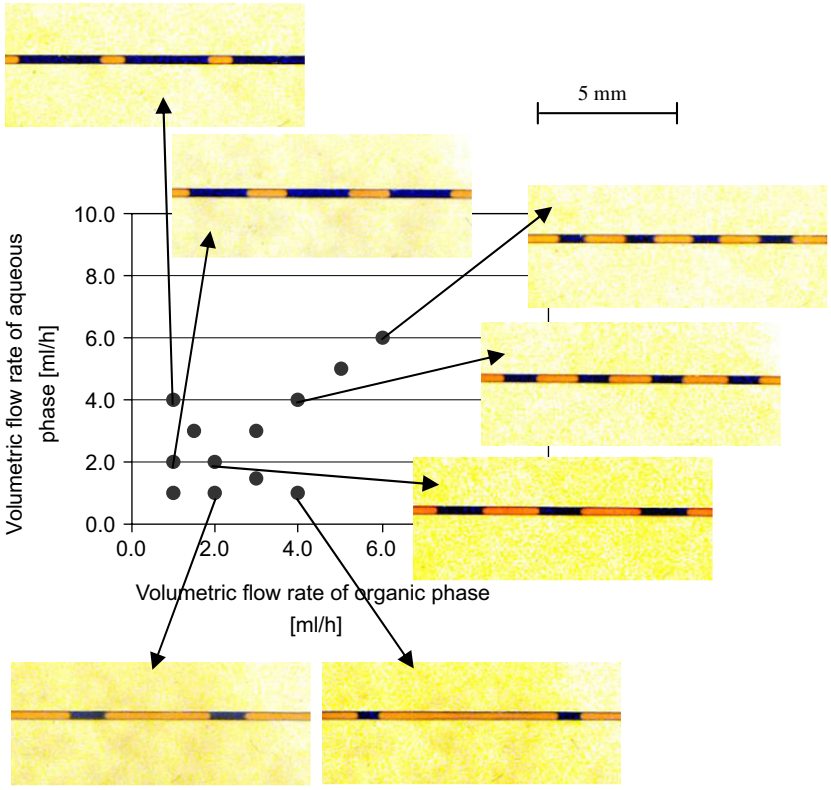

Fig. 3. Flow pattern map: example for the T-shaped microreactor. Organic phase = toluene with Sudan III. Aqueous phase = water with NaOH 0.15 M and bromothymol blue.

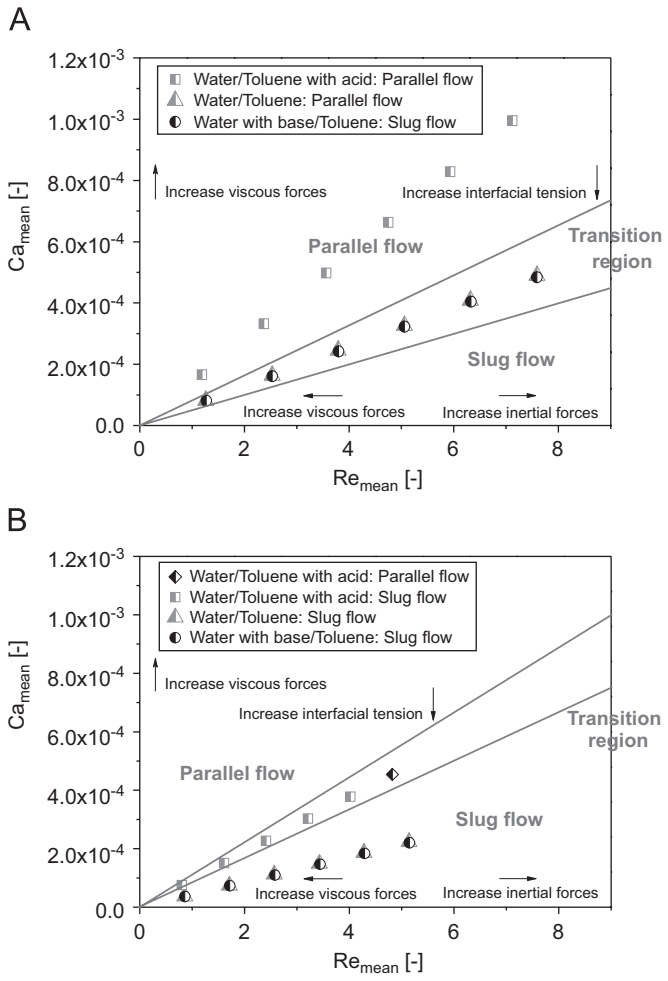

Fig. 4. Flow transition maps based on mean Capillary and mean Reynolds numbers for flow ratio of 1: (A) Y-shaped microreactor; (B) T-shaped microreactor.

reduces the interfacial area (Joanicot and Ajdari, 2005; Squires and Quake, 2005).

The acid addition in the organic phase increases the mean Capillary number in comparison to the water/toluene system. This means that the viscous forces increase in comparison to interfacial tension. Viscosity produces a resistance to shear (Atencia and Beebe, 2005) and the viscous stresses act to extend and drag the interface downstream (Joanicot and Ajdari, 2005; Squires and Quake, 2005). If the viscous stress is the main forces, a parallel flow will arise.

The increase of the mean Capillary number with the acid addition compared to the water/toluene system is big, but the decrease of mean Capillary number with the base addition as compared to the water/toluene system corresponds only to 1%. The Capillary and Reynolds numbers for the system with NaOH represent the stability limit for the two types of flow patterns.

For the T-shaped microreactor (Fig. 4B), the same trend was observed. Moreover, the effect of the linear velocity was observed for the acid system. An increase in the linear velocity leads to an increase in the viscous forces and produces the parallel flow.

As can be observed in Fig. 4, the inertia forces tend to produce slug flow. More precisely, inertia counters parallel movement creating turbulence. For all the experiments reported, the mean Weber numbers are smaller than 1. Therefore, the interfacial tension dominates the inertia forces producing slugs. Zhao et al. (2006) showed that if inertia forces dominate ($We > 10$), the turbulence appears and chaotic or annular flow are observed.

So, the observed flow patterns can be explained by a competition between the main forces due to interfacial tension and viscosity. Comparing two graphs in Fig. 4A and B, it can be seen that stability domains of flow patterns depend on the geometry of the microreactor: in the T-shaped microreactor the slug flow is easily obtained. These graphs allow predicting the flow patterns for known Reynolds and Capillary numbers if volumetric flow rates of the two phases are equal.

3.3. Mass transfer performance of parallel flow and slug flow

Based on the previous results, the Y-shaped microreactor was used to generate parallel flow and the T-shaped microreactor was

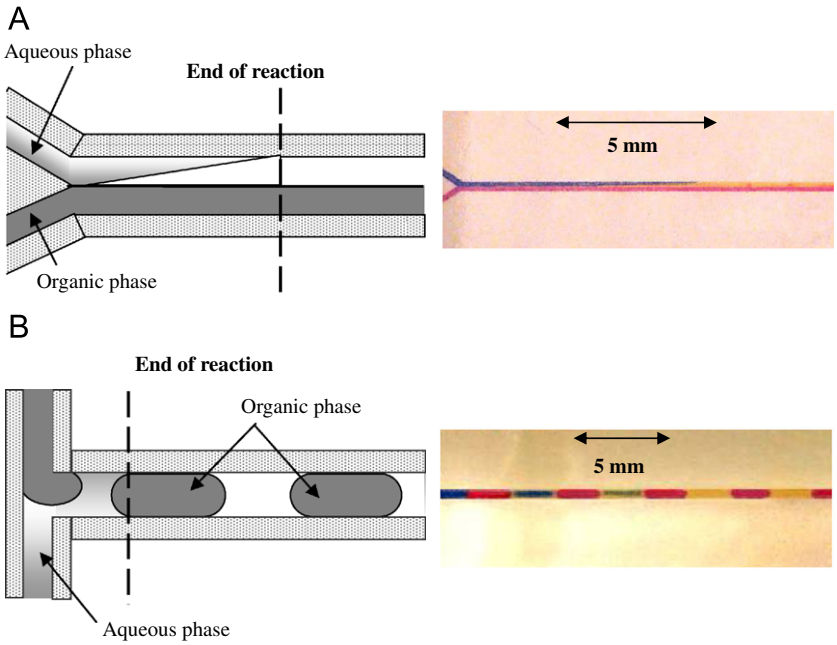

Fig. 5. (A) Neutralisation reaction with parallel flow. (B) Neutralisation reaction with slug flow (on the left a diagram and on the right a photograph).

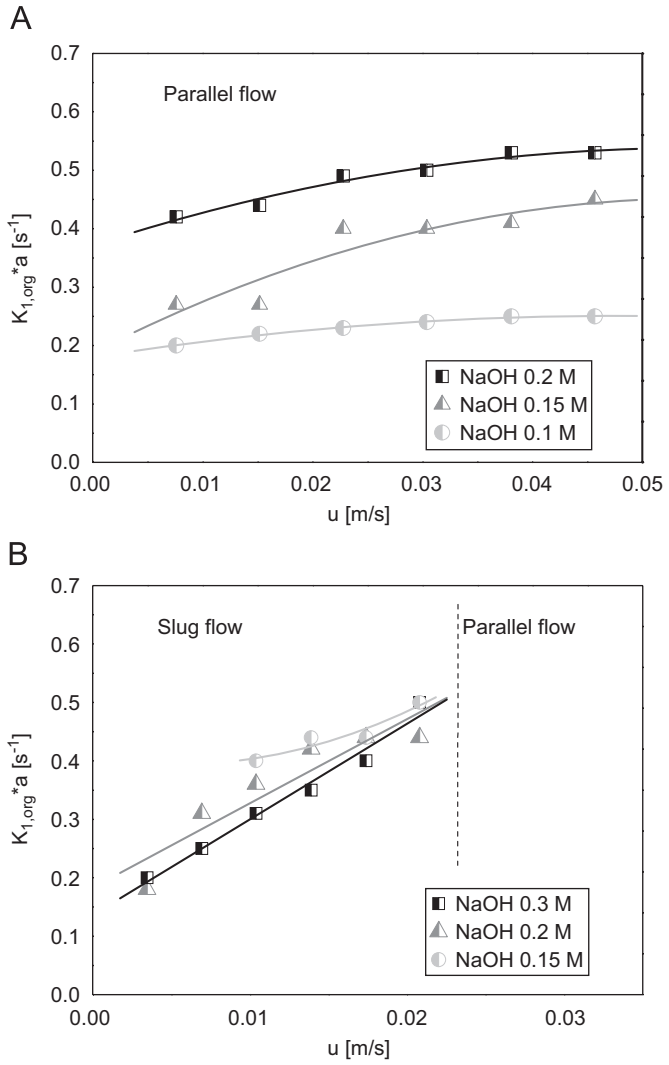

Fig. 6. Volumetric mass transfer coefficient in function of the linear velocity: (A) parallel flow. Organic phase=toluene with CCl_3COOH 0.6 M and Sudan III. Aqueous phase=water with NaOH and bromothymol blue. (B) Slug flow. Organic phase=hexane with CCl_3COOH 0.6 M and Sudan III. Aqueous phase=water with NaOH and bromothymol blue.

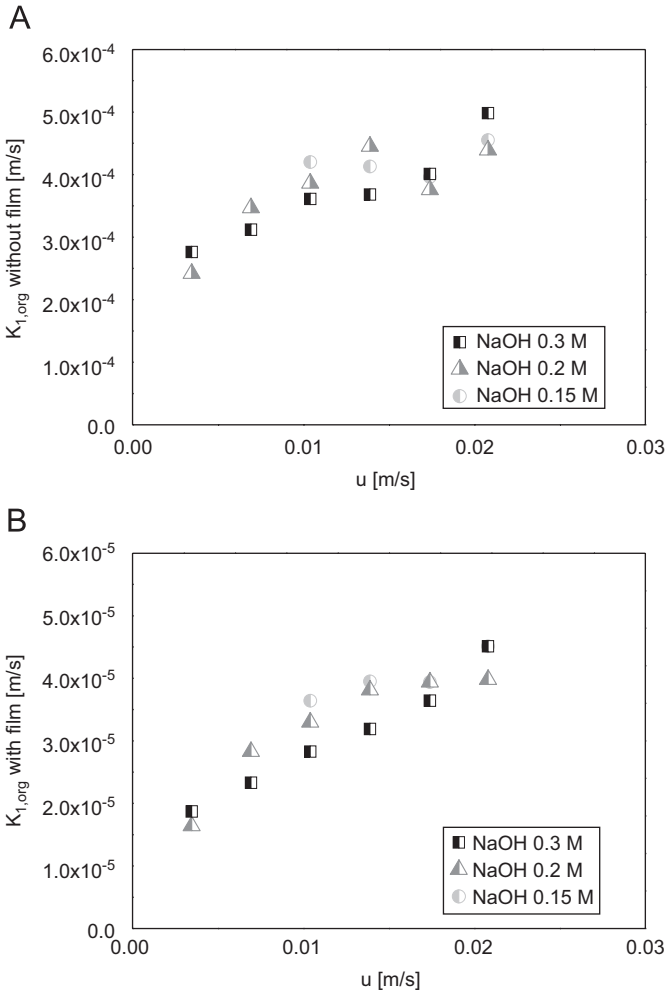

Fig. 7. Mass transfer coefficient in function of the linear velocity. (A) Slug flow without film. (B) Slug flow with film. Organic phase=hexane with CCl_3COOH 0.6 M and Sudan III. Aqueous phase=water with NaOH and bromothymol blue.

chosen as suitable to generate slug flow. In the case of a neutralisation reaction, the salt produced by the reaction also influences the flow pattern. To obtain stable slug flow in the T-shaped microreactor, the hexane/water system was used instead of toluene/water due to the higher interfacial tension. This was necessary in order to avoid non-defined flow patterns. These results confirm the importance of fluid properties on the flow pattern produced.

An example of the neutralisation reaction with parallel flow is shown in Fig. 5A. For parallel flow, the values of the global volumetric mass transfer coefficient ($K_{1,org} \cdot a$) range from 0.2 to 0.5 s^{-1}. They depend on the NaOH concentration and linear velocity (Fig. 6A). For the determination of the specific interfacial area, a flat interface in the middle of the channel was assumed. The specific interfacial area was calculated based on the volume of the organic phase. A constant value of 6850 m^{-1} was estimated. The resulting mass transfer coefficient is in the range of 3×10^{-5}–8×10^{-5} m/s for the parallel flow depending on the NaOH concentration and the linear velocity.

An example of the neutralisation reaction in a slug flow regime is shown in Fig. 5B. The global volumetric mass transfer coefficient was found to be approximately 0.2–0.5 s^{-1}. As shown in Fig. 6B, the volumetric mass transfer coefficient for slug flow depends on the linear velocity but not on the concentration of NaOH. The slug flow is not stable at flow velocities higher than 2×10^{-2} m/s. At these higher linear velocities, the parallel flow was observed.

Considering the case *without wall film formation*, the specific interfacial area was calculated assuming that the slugs have a rectangular shape and was referred to the volume of the organic phase in order to compare with the results reported in the literature (Burns and Ramshaw, 2001). The length of the slugs depends on the flow rate. So, the specific interfacial area increases with the linear velocity from 714 to 1176 m^{-1}. The resulting mass transfer coefficient is in the range of 2.5×10^{-4}–5×10^{-4} m/s (Fig. 7A). Burns and Ramshaw (2001) report mass transfer coefficients of the same order for slug flow in a capillary reactor of 0.38 mm diameter neglecting wall film formation. Considering *wall film formation*, the film thickness (h_f) can be estimated based on Bretherton's Law (Kashid et al., 2005):

$$h_f = 1.34 \cdot \frac{d_H}{2} \cdot Ca^{2/3} \tag{9}$$

A cylindrical shape was assumed for the calculation of the interfacial area and a value between 10,700 and 11,200 m^{-1} was obtained. The resulting mass transfer coefficient is in the range of 2×10^{-5}–4.5×10^{-5} m/s (Fig. 7B). In the case of slug flow, no influence of the NaOH concentration was observed on the mass transfer coefficient, but only the influence of the linear velocity was noticed.

The values of the volumetric mass transfer coefficient ($K_{1,org} \cdot a$) for the two microreactors are in the same range and are independent

of the flow pattern. The values for the mass transfer coefficients ($K_{1,org}$) are strongly dependent on the way used to estimate the specific interfacial area (a).

The obtained global volumetric mass transfer coefficients are in good agreement with the data reported in literature for the slug flow regime (liquid–liquid) in microreactors (Table 4). Similar mass transfer performance was also observed for a gas/liquid reaction in a microchannel. As can be seen in Table 4, the microreactors allow an increase in the global mass transfer coefficient of more than one order of magnitude as compared to conventional contactors and therefore, are powerful tools for the intensification of multiphase reactions.

The next chapter suggests a mechanism of the reaction in parallel flow and in slug flow regarding the influence of NaOH concentration and the linear velocity.

3.4. Modelling of instantaneous reaction

3.4.1. Parallel flow

The neutralisation reaction (Eq. (1)) in the aqueous phase is instantaneous and irreversible. Using a film model, the concentration profiles in the microreactor can be represented as shown in Fig. 8A, where y_{aqu} indicates the position of the reaction plane. As can be observed in Fig. 5A, the reaction plane within the aqueous phase moves towards the wall during the course of the reaction. This phenomenon is schematically shown in Fig. 8B.

The reaction can be presented in general form (Trambouze and Euzen, 2002):

$$\upsilon_1 A_1 + \upsilon_2 A_2 \rightarrow \upsilon_3 A_3 + \upsilon_4 A_4 \tag{10}$$

Reactants A_1 (CCl_3COOH) and A_2 (NaOH) have to diffuse from the interface and from the wall respectively to the reaction plane where both concentrations become zero. At steady state, the molar flows of acid $J_{1,aqu}$ and base $J_{2,aqu}$ must be equal:

$$J_{1,aqu} = -J_{2,aqu} \Rightarrow D_{1,aqu} \cdot \frac{C^*_{1,aqu}}{y_{aqu}} = D_{2,aqu} \cdot \frac{C_{2,aqu}}{(\delta_{aqu} - y_{aqu})} \tag{11}$$

The ratio between the film thickness δ_{aqu} and the position of the reaction plane y_{aqu} is given by:

$$\frac{\delta_{aqu}}{y_{aqu}} = 1 + \frac{D_{2,aqu} \cdot C_{2,aqu}}{D_{1,aqu} \cdot C^*_{1,aqu}} = E_i \tag{12}$$

The ratio corresponds to the enhancement factor for instantaneous reactions (E_i). The aqueous film mass transfer coefficient $k'_{1,aqu}$ in the case of absorption with chemical reaction is given by:

$$k'_{1,aqu} = k_{1,aqu} \cdot E_i \tag{13}$$

where $k_{1,aqu}$ corresponds to the aqueous film mass transfer coefficient in the case of physical absorption. As a consequence, the global mass transfer coefficient is given by:

$$\frac{1}{K_{1,org}} = \frac{1}{k_{1,org}} + \frac{m}{k_{1,aqu} \cdot E_i} \quad \text{(Hatta theory)} \tag{14}$$

So, the global mass transfer coefficient $K_{1,org}$ includes the resistance to mass transfer in both phases (Trambouze and Euzen, 2002).

With the reaction progress along the microchannel, the concentrations of NaOH and CCl_3COOH decrease and the reaction plane moves towards the wall. The enhancement factor E_i decreases due to the increase of the distance between reaction plane and the interface (Eq. (12) and Fig. 8B). Therefore, the mass transfer coefficient decreases with the distance as well. The mean value of the global mass transfer coefficient was measured.

The increase of the global mass transfer coefficient for the parallel flow was observed with increase of the initial concentration of NaOH at constant acid concentration. The initial acid concentration and, in consequence, the initial concentration at the interface, $C^*_{1,aqu}$, are the same and time independent for the different NaOH concentrations. According to the two-film theory, with increasing NaOH concentration in the aqueous phase, the enhancement factor E_i increases due to the decrease of the distance between reaction plane and the interface as illustrated in Fig. 8C. Therefore, the global mass transfer coefficient is increased and the mass transfer process is more efficient at higher NaOH concentration.

In liquid–liquid extraction systems the mass transfer process is traditionally rationalised using a two-film model. In the present study, the observed results for parallel flow were qualitatively described with this theory. However, due to the lack of information on the mass transfer coefficients without chemical reaction, the quantitative comparison of the results with Hatta theory was not possible. Analysis of the literature reports on liquid–liquid extraction accompanied by a neutralisation reaction showed that the mass transfer cannot always be explained on the basis of molecular diffusion only. Sherwood and Wei (1957) and Bakker et al. (1967) found mass transfer coefficients about three times higher than those predicted by the two-film and penetration theory and increased with the caustic concentrations. They proposed that the interfacial Marangoni instabilities are responsible for the high mass transfer rate observed. This spontaneous agitation of the interface appears due to fluctuations of temperature and concentrations resulting in local changes of the interfacial tension. The main reason for the enhancement of the mass transfer is an intense renovation of the interface. Pictorial diagram of interfacial turbulence has been suggested by Ruckenstein (1968) in the form of a roll-cell structure near the interface (Fig. 8D).

Most of the stability criteria related to Marangoni effects are derived for infinite liquid layers assuming mass transfer by diffusion only. Moreover, the effect of the chemical reaction is often not considered. Therefore, it is not possible to predict the existence of these instabilities in our system (Kovalchuk and Vollhardt, 2006). Further experiments are necessary to clarify this issue. If Marangoni instabilities are present, more complex interface models have to be applied (Mathpati and Joshi, 2007).

3.4.2. Slug flow

For the slug flow regime, the well-established hydrodynamics with internal circulations as described by Harries et al. (2003) and Kashid et al. (2005) is considered in this study (Fig. 9A). The mass transfer occurs via two distinct mechanisms: (a) convection due to the internal circulation in each slug; (b) molecular diffusion due to concentration gradients between adjacent slugs.

Two limiting cases have been considered: (i) the diffusion dominates and convection is negligible and (ii) the convection dominates and diffusion can be neglected. In the case of diffusion regime, the fluid is supposed to be stagnant in each slug. The mass transfer process can be represented using a two-film model as shown in Fig. 9C for a given axial position. For convection regime, a complete mixing is supposed in each slug. In this case, the hydrodynamic boundary layer strives towards zero (Fig. 9D).

The observation of the reaction in slug flow (Fig. 9B) shows that the concentration is not homogenous in the slugs suggesting an intermediate hydrodynamics involving diffusion and convection. In the slug flow regime, the hydrodynamic boundary layer is limited to a region very close to the interface due to the internal circulation. Moreover, the concentration in the bulk of the slug is not constant as in the case of a complete mixing. Due to the presence of stagnant and recirculation zones, the concentration of NaOH in the bulk of the slug varies as observed in Fig. 9B.

The main feature observed for a slug flow is that the mass transfer coefficient does not depend on the NaOH concentration.

Table 4
Mass transfer data for microsystems and conventional contactors

	Regime and system	Conditions	Global volumetric mass transfer coefficient
Liquid–liquid system in microreactors			
Burns and Ramshaw (2001)	• Slug flow • Reacting system Kerosene/acetic acid/water+NaOH	$d_H = 380\,\mu m$ $C_{\text{acetic acid,org}} = 0.65\,M$ $C_{\text{NaOH,aqu}} = 0.1–0.4\,M$ $u = 0–35\,mm/s$	Order of magnitude of $0.5\,s^{-1}$
Kashid et al. (2007)	• Slug flow • Nonreacting systems Kerosene/acetic acid/water, …	$d = 0.5–1\,mm$ $C_{\text{acetic acid,org}} = 0.03\,M$ $u = 10–70\,mm/s$	$\sim 0.4–0.8\,s^{-1}$ ($u = 10–30\,mm/s$)
Present study	• Slug flow • Reacting system Hexane/ trichloroacetic acid/water+NaOH	$d_H = 400\,\mu m$ $C_{\text{acid,org}} = 0.6\,M$ $C_{\text{NaOH,aqu}} = 0.15–0.3\,M$ $u = 0–20\,mm/s$	$0.2–0.5\,s^{-1}$
Present study	• Parallel flow Reacting system Toluene/trichloroacetic acid/water+NaOH	$d_H = 269\,\mu m$ $C_{\text{acid,org}} = 0.6\,M$ $C_{\text{NaOH,aqu}} = 0.1–0.2\,M$ $u = 0–50\,mm/s$	$0.2–0.5\,s^{-1}$
Gas–liquid system in microreactors			
Yue et al. (2007)	• Slug flow • Reacting system CO_2/buffer solution of $NaHCO_3$ and Na_2CO_3	$d_H = 667\,\mu m$ $u_L = 0.09–1\,m/s$ $u_G = 0–2\,m/s$	Liquid side volumetric mass transfer coefficient in the order of $0.3–0.5\,s^{-1}$ ($u_L = 0.09\,m/s$)
Conventional contactors for liquid–liquid systems			
Spray column[a]	• Nonreacting system Water/acetic acid/benzene		$\sim (1.75–6.3) \times 10^{-3}\,s^{-1}$
Impinging streams[a]	• Nonreacting system Kerosene/acetic acid/water		$\sim 0.05–0.3\,s^{-1}$

[a]Data found in Kashid et al. (2007).

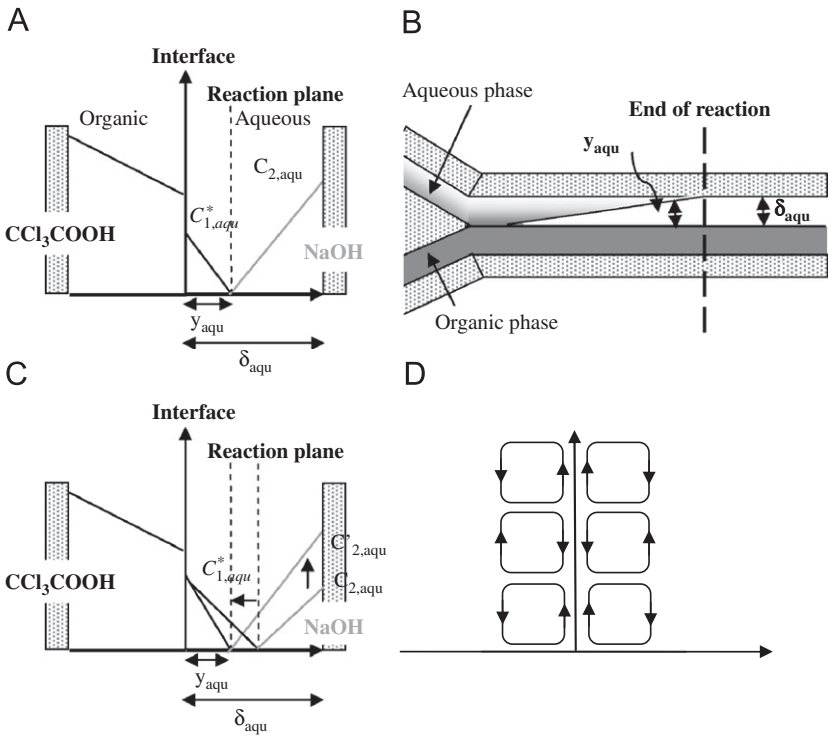

Fig. 8. (A) Schematic presentation of the concentration profiles according to the film model in the case of an instantaneous reaction in parallel flow. (B) Schematic presentation of the observed evolution of the reaction plane in the microchannel. (C) Influence of the initial NaOH concentration on the concentration profile in the aqueous phase. (D) The roll-cell model as proposed by Ruckenstein (1968).

Due to the internal circulation in slug flow, the hydrodynamic boundary layer is reduced and the influence of the NaOH concentration, as predicted by the Hatta theory, is not observed. Moreover, this experimental result indicates that for the conditions of the experiments, the Marangoni instabilities are very weak or not present.

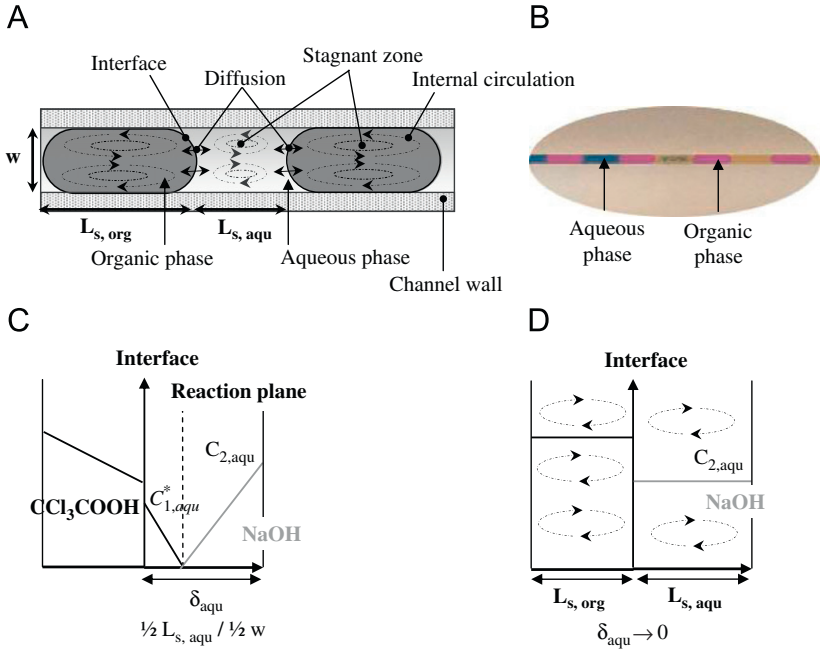

Fig. 9. (A) Hydrodynamics of slug flow. (B) Photo of slug flow observed. (C) Concentration profile for the assumption of stagnant slugs (diffusion regime). (D) Concentration profiles for complete mixing in the slugs (convection regime).

The increase of the volumetric mass transfer coefficient ($K_{1,org} \cdot a$) with the linear velocity (Fig. 6B), in the case of slug flow, can be explained by two distinct effects: (a) the increase of the interfacial area, (b) the increase of the internal circulation. An increase of the linear velocity leads to a decrease of the length of the slugs and therefore, to an increase of the interfacial area. Moreover, the increase of the linear velocity increases the internal circulation within the slugs resulting in the higher mass transfer observed.

4. Conclusions

- The influence of fluid properties on the formation of liquid–liquid two-phase flow patterns and the mass transfer performance between two immiscible liquids were investigated for T- and Y-shaped glass microreactors using deionised water and dyed toluene (or hexane).
- The formation of slug and parallel flow is controlled by the competition between the viscous forces and the interfacial tension. A model based on the mean Capillary and Reynolds numbers was developed. This model allows predicting the dependence of the flow patterns on the fluid properties.
- The mass transfer performance was studied using instantaneous neutralisation reaction. For the conditions applied during the study, the slug flow and parallel flow showed similar mass transfer performance with the global mass transfer coefficient in the range of 10^{-5}–10^{-4} m/s. For the parallel flow, the mass transfer coefficient was mainly affected by the base concentration in water. For the slug flow, the main parameter was the linear velocity. The prediction of the mass transfer coefficient remains difficult due to secondary phenomena, like interfacial instabilities, which have not been fully understood.
- The results obtained are important for the design of microreactors to carry out multiphase chemical reactions aiming on process intensification.

Notation

a	specific interfacial area, m^2/m^3
$C_{i,I}$	molar concentration of species i in phase I, mol/m^3
d	diameter of the channel, m
d_H	hydraulic or equivalent diameter of the channel, m
$D_{i,I}$	molecular diffusivity, m^2/s
E_i	enhancement factor for instantaneous reaction, dimensionless
g	gravitational constant, m/s^2
h_f	wall film thickness, m
H	height, m
$J_{i,I}$	molar flux of species i in phase I, $mol/m^2/s$
$k_{i,I}$	mass transfer coefficient of the film I for species i, m/s
$K_{i,I}$	global mass transfer coefficient of species i referred to phase I, m/s
Ls	length of slugs, m
m	slope of the equilibrium relation between concentration, dimensionless
Q_I	volumetric flow rate of phase I, m^3/s
R_i	rate of transformation of species i, $mol/m^3/s$
u	linear or superficial velocity, m/s
w	width, m
y_I	distance interface—reaction plane in phase I, m

Greek letters

δ_I	hydrodynamic boundary layer in phase I, m
μ	dynamic fluid viscosity, Pa s or kg/m/s
ρ	fluid density, kg/m^3
σ	interfacial tension or liquid–liquid surface tension, kg/s^2 or N/m
τ_R	reaction time, s
υ	stoichiometric coefficient, dimensionless

Subscripts

E	equilibrium
i	species: 1 = CCl_3COOH; 2 = NaOH
I	phase: org = organic phase; aqu = aqueous phase
0	initialconditions
$*$	interfacial

Acknowledgements

Financial support by the Swiss National Science Foundation and the Swiss Commission for Technology and Innovation (CTI) is gratefully acknowledged.

References

Ahmed, B., Barrow, D., Wirth, T., 2006. Enhancement of reaction rates by segmented fluid flow in capillary scale reactors. Advanced Synthesis and Catalysis 348, 1043–1048.

Akbar, M.K., Plummer, D.A., Ghiaasiaan, S.M., 2003. On gas–liquid two-phase flow regimes in microchannels. International Journal of Multiphase Flow 29, 855–865.

Atencia, J., Beebe, D.J., 2005. Controlled microfluidic interfaces. Nature 437, 648–655.

Bakker, C.A.P., Fentener van Vlissingen, F.H., Beek, W.J., 1967. The influence of the driving force in liquid–liquid extraction—a study of mass transfer with and without interfacial turbulence under well-defined conditions. Chemical Engineering Science 22, 1349–1355.

Burns, J.R., Ramshaw, C., 1999. Development of a microreactor for chemical production. Transactions of the Institution of Chemical Engineers 77, 206–211.

Burns, J.R., Ramshaw, C., 2001. The intensification of rapid reactions in multiphase systems using slug flow in capillaries. Lab on a Chip 1, 10–15.

Burns, J.R., Ramshaw, C., Harston, P., 1998. Development of a microreactor for chemical production. Topical Conference Preprints: Process Miniaturization-IMRET2: 2nd International Conference on Microreaction Technology, New Orleans, Louisiana, pp. 39–44.

Dummann, G., Quittmann, U., Gröschel, L., Agar, D.W., Wörz, O., Morgenschweis, K., 2003. The capillary-microreactor: a new reactor concept for the intensification of heat and mass transfer in liquid–liquid reactions. Catalysis Today 79–80, 433–439.

Ehrfeld, W., Hessel, V., Löwe, H., 2000. State of the art of microreaction technology. Microreactors: New Technology for Modern Chemistry. Wiley-VCH, Weinheim. pp. 1–14.

Harries, N., Burns, J.R., Barrow, D.A., Ramshaw, C., 2003. A numerical model for segmented flow in a microreactor. International Journal of Heat and Mass Transfer 46, 3313–3322.

Hessel, V., Löwe, H., 2005. Organic synthesis with microstructured reactors. Chemical Engineering and Technology 28, 267–284.

Jähnisch, K., Hessel, V., Löwe, H., Baerns, M., 2004. Chemistry in microstructured reactors. Angewandte Chemie International Edition 43, 406–446.

Joanicot, M., Ajdari, A., 2005. Droplet control for microfluidics. Science 309, 887–888.

Kashid, M.N., Agar, D.W., 2007. Hydrodynamics of liquid–liquid slug flow capillary microreactor: flow regimes, slug size and pressure drop. Chemical Engineering Journal 131, 1–13.

Kashid, M.N., Gerlach, I., Goetz, S., Franzke, J., Acker, J.F., Platte, F., Agar, D.W., Turek, S., 2005. Internal circulation within the liquid slugs of a liquid–liquid slug-flow capillary microreactor. Industrial and Engineering Chemistry Research 44, 5003–5010.

Kashid, M.N., Harshe, Y.M., Agar, D.W., 2007. Liquid–liquid slug flow in a capillary: an alternative to suspended drop or film contactors. Industrial and Engineering Chemistry Research 46, 8420–8430.

Kiwi-Minsker, L., Renken, A., 2005. Microstructured reactors for catalytic reactions. Catalysis Today 110, 2–14.

Kovalchuk, N.M., Vollhardt, D., 2006. Marangoni instability and spontaneous nonlinear oscillations produced at liquid interfaces by surfactant transfer. Advances in Colloid and Interface Science 120, 1–31.

Kreutzer, M.T., Kapteijn, F., Moulijn, J.A., Heiszwolf, J.J., 2005. Multiphase monolith reactors: chemical reaction engineering of segmented flow in microchannels. Chemical Engineering Science 60, 5895–5916.

Lide, D.R. (Ed.). 2007. CRC Handbook of Chemistry and Physics, Internet Version 2007, 87th ed. Taylor and Francis Boca Raton, FL ⟨http://www.hbcpnetbase.com⟩.

Lomel, S., Falk, L., Commenge, J.M., Houzelot, J.L., Ramdani, K., 2006. The microreactor. A systematic and efficient tool for the transition from batch to continuous process. Transactions of the Institution of Chemical Engineers, Part A, Chemical Engineering Research and Design 84, 1–7.

Löwe, H., Ehrfeld, W., 1999. State-of-the-art in microreaction technology: concepts, manufacturing and applications. Electrochimica Acta 44, 3679–3689.

Mathpati, C.S., Joshi, J.B., 2007. Insight into theories of heat and mass transfer at the solid–fluid interface using direct numerical simulation and large Eddy simulation. Industrial and Engineering Chemistry Research 46, 8525–8557.

Ruckenstein, E., 1968. Mass transfer in the case of interfacial turbulence induced by the Marangoni effect. International Journal of Heat and Mass Transfer 11, 1753–1760.

Sherwood, T.K., Wei, J.C., 1957. Interfacial phenomena in liquid extraction. Industrial and Engineering Chemistry 49, 1030–1034.

Squires, T.M., Quake, S.R., 2005. Microfluidics: fluid physics at the nanoliter scale. Reviews of Modern Physics 77, 977–1026.

Thorsen, T., Roberts, R.W., Arnold, F.H., Quake, S.R., 2001. Dynamic pattern formation in a vesicle-generating microfluidic device. Physical Review Letters 86, f 4163–4166.

Tice, J.D., Lyon, A.D., Ismagilov, R.F., 2004. Effects of viscosity on droplet formation and mixing in microfluidic channels. Analytica Chimica Acta 507, 73–77.

Trambouze, P., Euzen, J.-P., 2002. Les Réacteurs chimiques; De la conception à la mise en oeuvre. Ed. Technip, Paris.

Vazquez, G., Alvarez, E., Varela, R., Cancela, A., Navaza, J.M., 1996. Density and viscosity of aqueous solutions of sodium dithionite, sodium hydroxide, sodium dithionite+sucrose, and sodium dithionite+sodium hydroxide+sucrose from 25 °C to 40 °C. Journal of Chemical and Engineering Data 41, 244–248.

Weast, R.C., Ed., 1971. CRC Handbook of Chemistry and Physics. 52nd ed. Chemical Rubber, Cleveland, OH.

Yue, J., Chen, G., Yuan, Q., Luo, L., Gonthier, Y., 2007. Hydrodynamics and mass transfer characteristics in gas–liquid flow through a rectangular microchannel. Chemical Engineering Science 62, 2096–2108.

Zhao, Y., Chen, G., Yuan, Q., 2006. Liquid–liquid two-phase flow patterns in a rectangular microchannel. A.I.Ch.E. Journal 52, 4052–4060.